Landslides (2004) 1:203–209
DOI 10.1007/s10346-004-0029-x
Received: 6 April 2004
Accepted: 4 August 2004
Published online: 4 September 2004

Masahiro Chigira · Fengjun Duan · Hiroshi Yagi · Takahiko Furuya

Using an airborne laser scanner for the identification of shallow landslides and susceptibility assessment in an area of ignimbrite overlain by permeable pyroclastics

Abstract An airborne laser scanner can identify shallow landslides even when they are only several meters in diameter and are hidden by vegetation, if the vegetation is coniferous or deciduous trees in a season with fewer leaves. We used an airborne laser scanner to survey an area of the 1998 Fukushima disaster, during which more than 1,000 shallow landslides occurred on slopes of vapor-phase crystallized ignimbrite overlain by permeable pyroclastics. We identified landslides that have occurred at the 1998 event and also previous landslides that were hidden by vegetation. The landslide density of slopes steeper than 20° was 117 landslides/km^2 before the 1998 disaster. This event increased the density by 233 landslides/km^2 indicating that this area is highly susceptible to shallow landsliding.

Keywords Laser scanner · Landslide · Rainstorm · Susceptibility mapping · Fukushima, Japan

Introduction

Because surface instability is generally reflected in geomorphological features, geomorphology gives us clues we can use to extract existing and potential sites of slope movement from a wide area or to assess hazard potential of a given area. We can observe geomorphological features in a wide area in a consistent manner from the air, but humid areas like Japan are covered by thick forest, and even after tree leaves are gone, the ground surface is not easily seen from the air. This has been a significant obstacle to investigating a wide area for small geomorphic features that provide essential information in the making of landslide inventory maps and assessing susceptibility to slope movement. On the other hand, airborne laser altimetry surveys that have been used recently to analyze geomorphic features such as the deformation of volcanoes, forest canopy structures, and so on, could be used to monitor the ground surface by radiating laser beams that penetrate forest canopies through open interstices.

We applied the airborne laser altimetry technique to the Nishigo area of the Fukushima rainstorm disaster, which occurred from 26 to 31 August 1998. More than 1,000 landslides occurred on slopes consisting of vapor-phase crystallized ignimbrite overlain by scoria, pumice, and ash. The geology and the types of landslides that occurred were reported previously (Chigira 2002; Chigira et al. 2002). Here we describe the geomorphic features of the landslides and discuss how to locate previous landslides and to assess the susceptibility to landslide in this area by using laser altimetry. During the time of this disaster, five people were killed before dawn in a welfare house. This disaster and the following disaster in Hiroshima in 1999 became a turning point for the Japanese government in preparing a new law regarding disaster prevention against slope movement hazard.

Airborne laser scanning—airborne scanning laser altimetry, or LiDAR (light-induced direction and ranging)—has been applied to various geomorphic or geologic issues during this decade, including the deformation of volcanoes (Ridgway et al. 1997), flood damage (Bates et al. 2003), ice-sheets budget (Kennet and Eiken 1997), geomorphological and hydraulic modeling (French 2003; Lane et al. 2003), landslide susceptibility (Montgomery et al. 2000), and landslide morphology (McKean and Roering 2004). Montgomery et al. (2000) used a map made by laser altimetry to study a shallow landslide, however the map was not used to identify the landslide itself, but was instead only used to make a digital elevation model (DEM).

Hazard mapping of landslides and susceptibility assessment of a given area have been urgent issues in mitigating natural disasters, but their methodology is not established as yet. There have been two approaches: one is a deterministic approach represented by the analysis of infinite slope stability using a hydrologic/stability model introducing geotechnical and hydrological parameters (Okimura and Kawatani 1987; Montgomery and Dietrich 1994; Wu and Sidle 1995); another is based on the stochastic model-like usage of logistic regression involving past landslides, geology, slope gradient, land cover, and the like (Carrara et al. 1991; Gupta and Joshi 1997; Dai and Lee 2003). The former approach has unavoidable problems in the variability of parameters, which varies from place to place according to various soil structures. Logistic regression and other statistical techniques also has problems in the identification of landslides; it works easily for new landslides but does not work as well for old ones obscured by vegetation when using traditional aerial photographs or satellite images. In addition, identified landslides are located on maps made from aerial photographs, and these maps are too rough to be used for the geomorphic characterization of shallow landslides. This paper focuses on the extraction of old landslides as well as new ones by using laser technique, which leads to regional susceptibility evaluation rather than the evaluation of local, specific slopes.

Method

We identified landslides that occurred during the 1998 disaster on aerial photographs with a scale of 1:8,000 and also by ground-truth geological investigation (Chigira 2002; Chigira et al. 2002). Airborne laser scanning was performed for an area of 2.5 km^2 within the 1998 disaster area of Fukushima in late April, 2002 (Fig. 1). The system used was ALTM1225. The ALTM sensor aboard an AS350B helicopter operated at 25,000 pulses/s at a wavelength of 1,064 nm with scanning angles of 10–20°. This technique provides highly precise horizontal (approximately 0.5 m) and vertical (approximately 0.15 m) height locations. Using this data, we made a 1-m grid Digital Terrain Model (DTM) and a topographic map with 1-m contour intervals.

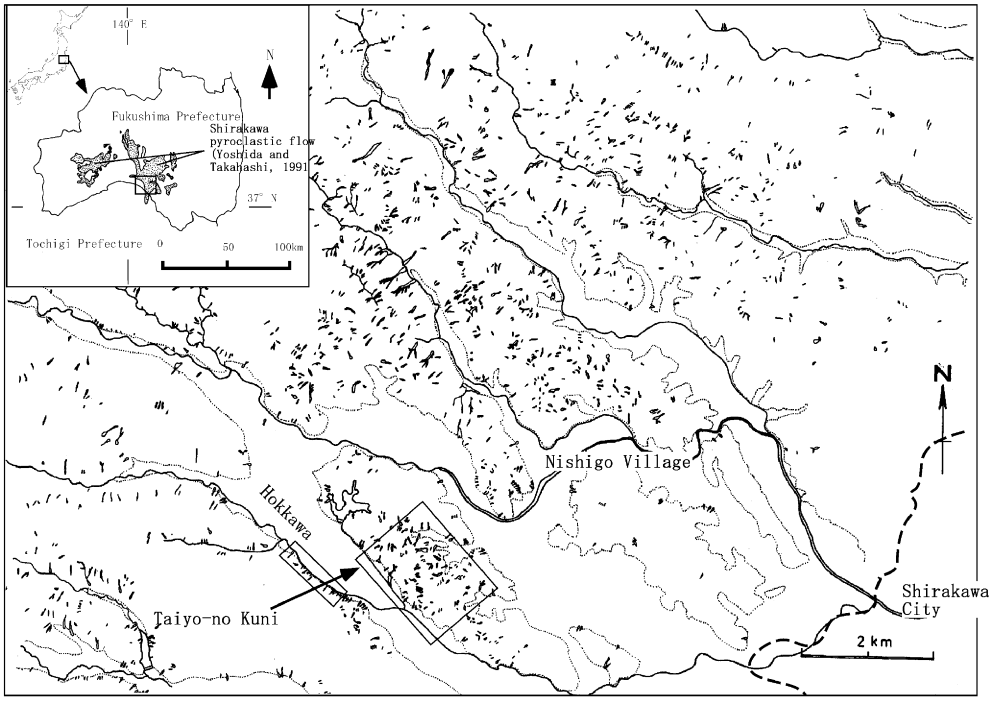

Fig. 1 Index map and landslide distribution. The areas measured by airborne laser scanner are shown by *two squares*

Geology and geomorphology

Small plateaus, about 60–100 m high above the nearby fluvial plains, occupy a wide area in and around Nishigo Village. The tops of the plateaus are essentially depositional surfaces of pyroclastic flow covered by thin tephra layers. The bedrock of the plateaus is the early Quaternary Shirakawa pyroclastic flow (Yoshida and Takahashi 1991; Suzuki et al. 1998) overlain by thin beds of pyroclastics, which are thought to have erupted from Nasu Volcano 200,000–350,000 years ago (Suzuki 1992). The Shirakawa pyroclastic flow has been divided into several flow units, and the flow in and around the investigated area has been fission track dated to 780 ka (Suzuki et al. 1998) and consists of dacitic ignimbrite (tuff), which is a weakly consolidated, massive, and intact tuff that had been subjected to vapor-phase crystallization (Chigira et al. 2002). This vapor-phase crystallized tuff has a characteristic weathering profile that consists of hydrated, exfoliated, and disintegrated zones toward the ground surface (Chigira et al. 2002). The tuff of the hydrated zone is significantly deteriorated but is still massive. The tuff of the exfoliated zone is exfoliated to slope-parallel plates or lenses a few to 5 cm thick. The disintegrated tuff has lost its original rock structure and is soil-like.

The tephra layers overlying the Shirakawa pyroclastic flow are exposed in landslide scars and artificial cuttings; elsewhere they are covered by vegetation. These beds, which consist of mudflow deposits (diamicton made up of tuffaceous fines and andesite blocks) and air-fall deposits of scoria, orange or white pumice, and ash, are nearly horizontal, hence their outcrop traces fall along contour lines. The thicknesses of the mudflow deposits vary from 2 - 20 m. The total thickness of the scoria and pumice beds varies from 0.5 - 3.5 m, and the thickness of the ash occupying the top of the plateau is not precisely known but is estimated to be up to 10 m. The permeability of the underlying tuff is very low in comparison with the overlying tephra layers, which was one of the major causes of the landslides (Chigira 2002).

Geomorphological and geological features of the landslides generated by the 1998 rainstorm and previous landslides

Aerial photographs taken from 10 to 11 September 1998 revealed that 203 landslides occurred within the laser-scanned area at the time of this disaster, but it is not easy to recognize whether previous landslide scars were present or not on the aerial photographs (Fig. 2A). The laser scanner map, however, clearly shows previous landslide scars as well as those during this event (Fig. 2B, C). One hundred and two previous landslide scars are identified on the basis of morphological characteristics, which will be described below (Fig. 3).

As has been reported by Chigira (2002) and Chigira et al. (2002), three types of landslides occurred during this disaster, including landslides of pyroclastic deposits overlying weakly consolidated ignimbrite, landslides of weathered tuff and colluviums, and landslides of depression fill. These types of landslides strongly reflected the hydrogeological structure. The typical morphology of these landslides is shown as laser-scanner maps and profiles in Fig. 4, in which profiles made by the laser scanner and by survey are both shown. These morphological characteristics will be described in the following sections. The differentiations of landslide types were made by the field investigation of a limited number (approximately 50) of landslides, and not all landslides shown in Fig. 3 have been differentiated (Chigira 2002).

Landslides of pyroclastic deposits overlying weakly consolidated ignimbrite

Landslides of pyroclastic deposits overlying weakly consolidated ignimbrite involve pyroclastic air-fall deposits overlying diamicton of mudflow deposits on weakly consolidated ignimbrite as well

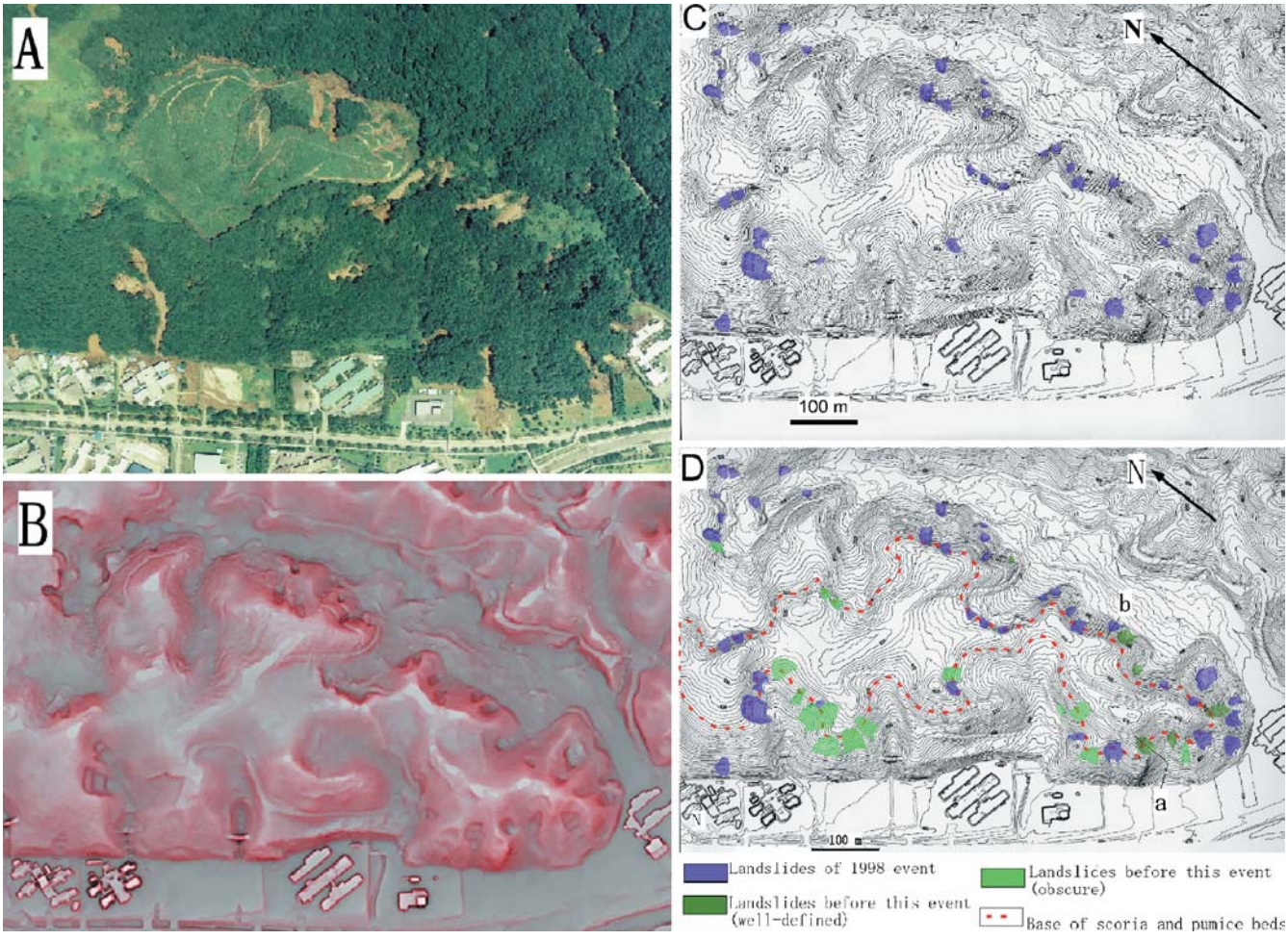

Fig. 2 **A** Aerial photograph, **B** red three-dimensional image (by Asia Air Survey, Co.), **C** laser scanner map and **D** landslide distribution mapped on the laser scanner map. Aerial photograph was taken by Kokusai Kogyo Co. from 10 to 11 September, 1998. Contour interval is 1 m. Cross sections along *two lines* in **D** (*a*, *b*) are shown in Fig. 4

as debris on top. They were aligned along the trace of the pumice and scoria beds on gentle convex breaks along the periphery of the small plateaus (Figs. 2D and 3). Figure 2 indicates the base of the pumice and scoria beds and Fig. 3 also indicates it as well as the base of underlying mudflow deposits, which varies in thickness and locally is almost lacking. At these slope breaks, the flat top surfaces of the plateaus gradually change to the lower slopes, which incline 20–30°. This type of landslide occurred because of the vertical contrast of hydraulic conductivities. The hydrated tuff, which forms the top of the massive and weakly weathered tuff and underlies the less permeable mudflow deposits, is impermeable, and most of the air-fall deposits are highly permeable except for white pumice tuff, which is a few tens of centimeters up to 1 m thick just above the mudflow deposits and is sometimes lacking. The exfoliated zone of the tuff is usually less than 1 m thick. The disintegrated zone of the tuff is present generally beneath the slope surface and is missing just beneath mudflow deposits. This hydrogeological structure, which is permeable beds overlying impermeable rock, affected the infiltrating behavior of rainwater; rainwater on small plateaus first infiltrates vertically and then flows laterally within permeable air-fall deposits, finally gushing out at the periphery of the plateaus to cause landslides.

The geometry of this type of landslide is clearly shown on a map made by a laser scanner (Fig. 4A). The landslide shown in Fig. 4A, however, is an old one because new landslide scars had been artificially modified at the time of laser scanning. The landslide scar of this type of landslide is a characteristic amphitheater or bowl-like depression, of which morphology resulted from the landslide generated by the gushing out of water. The size of the bowl varies from 5 to 15 m in diameter and a few to 5 m in depth. Mudflow deposits usually are exposed at the bottom of the bowl, and air-fall deposits crop out in the upper part of the scar. The lower part of the bowl is very gentle and inclines from 5 to 15° and the upper part inclines from 30° to 45°. The height of the head scarps varied from a few to 5 m.

The laser-scanner map clearly indicates that this type of landslide was aligned along the trace of the air-fall deposits: 39 new landslides and 21 previous landslides were identified as being aligned along a part of the 5.14-km trace of the pumice and scoria beds (Fig. 3), indicating that this type of landslide had occurred before the 1998 event to slopes with the same hydrogeological structure. Those landslides sites that occurred before the 1998 event are vegetated again and their deposits can hardly be recognized, probably because they were easily eroded by water.

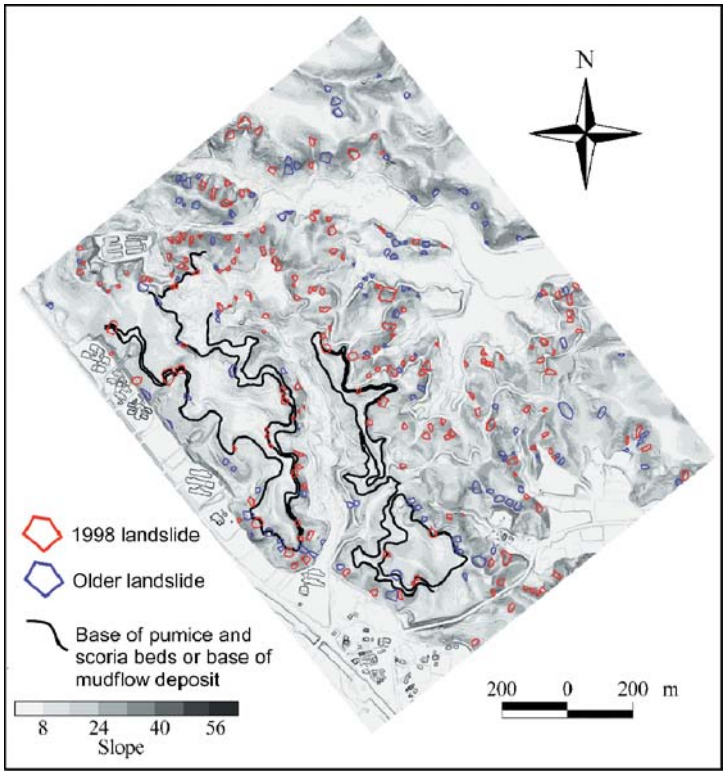

Fig. 3 Landslides identified by the laser scanner map before and after the 1998 disaster. Trace of the base of pumice and scoria beds and mud flow deposits are shown

Whether the landslides that occurred in 1998 were preceded by previous landslides is not known, because we have no laser-scanner map of this area before this study.

Close inspection of the laser-scanner map suggests that the hydrogeological structure providing the basic cause of this type of landslide formed a 10–20-m-wide terrace-like landform in some locations (Fig. 5, east part of Fig. 3). This terrace-like surface approximately coincides with the trace of the mudflow deposits just above the ignimbrite and beneath the air-fall deposits. In addition, mudflow deposits were generally exposed at the base of the lower part of the bowl-like landslide scars, and the lower part of these landslides was very gentle. These facts suggest that the terrace-like landform is the result of landslides along the trace of the air-fall pyroclastics and the retrogression of the landslide scars by repetitive shallow landslides of this type. Such terrace-like morphology suggests the hydrogeological structure of permeable materials on impermeable material and may indicate a high potential for this type of landslide. This landform is also due to the weak air-fall pyroclastics and mudflow deposits on comparatively hard, weakly consolidated ignimbrite.

Landslides of weathered tuff and colluvium

This type of landslide occurred on weakly consolidated ignimbrite with the sliding surface within the exfoliated zone, which forms the bottom of the intensively weathered zone (Chigira et al. 2002). This type of landslide stripped away most of the slide material, leaving a bright-colored rock surface of an exfoliated zone at the landslide scar. The scars dip 25–45° with an average of 32°, from a few to 5° steeper than the juxtaposing slope. This is because on the lower part of the slope, debris is generally accumulated on the rock surface. The landslide scar has a planar base along the exfoliated zone with a U-shaped scarplet upslope (Fig. 4B), which is in contrast to the bowl-like morphology of the landslide scars of air-fall pyroclastics on the mudflow and the ignimbrite, as is shown in contour maps and cross sections made by the air-born laser scanner. The morphology of this scar also clearly indicates its landslide origin. In comparison with the cross section made by ground survey, the cross section made from the laser scanner shows a somewhat rounded edge at the top of the landslide scarplet, but the shape of the landslide scar can generally be clearly detected. The size of the scar varies from 5 to 30 m in width and length and less than a few meters in depth.

The basic causes of this type of landslide were three factors: the weathering front of the tuff is clearly defined with large reduction of strength; the tuff has few primary cracks so that groundwater does not infiltrate further downward from the weathering front; and plant roots do not penetrate into its intact part to support the surface material. The tuff with these mechanical and hydrogeological properties was hit by a rainstorm, and weathered layers were presumably saturated with water and slid.

Landslides of depression fill

The intense rainfall also triggered failure of colluvium or ash that filled depressions, although this type of failure seemed less common than the other two types. A typical example of this was a landslide that occurred near Daishin Junior High School, 15 km northeast of Taiyo-no Kuni, where a former buried stream was exposed again by the landslide, leaving a scar of 5-m deep and 80-m long (Umemura et al. 1999; Chigira 2002). The hollow upslope of this landslide had old depressions a few meters in diameter and less than 1-m deep, indicating that underground erosion and ground settlement preceded the landslide. The gradient of this hollow before the slide is assumed to be 15° based on a survey

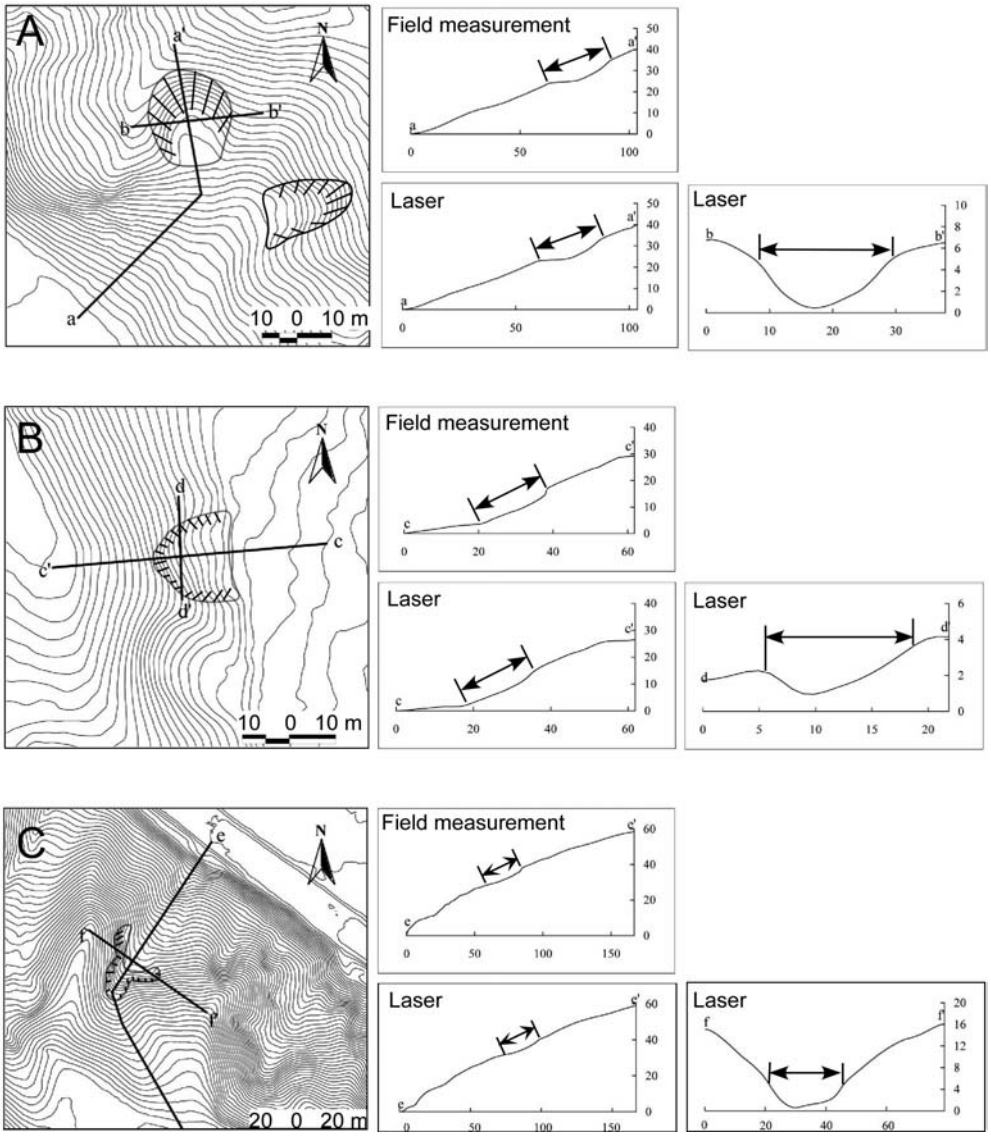

Fig. 4 Typical morphology of three types of landslides shown by contour maps and cross sections that were made from contour maps and ground survey. Contour interval is 1 m. *Arrows* indicate the area of landslide scar **A** Landslide of pyroclastic deposits overlying weakly consolidated ignimbrite; **B** landslide of weathered tuff and colluviums; **C** landslide of depression fill. Locations of **A** and **B** are shown in Fig. 2, and the location of **C** is on the south bank of the Hokkawa River (Fig. 1). See text for details. The locations of **A** and **B** are shown in Fig. 2

made after the slide (Umemura et al. 1999). In addition, this old depression fill was cut artificially for construction at the lower part of the slope, and this landslide seems to have started at this cutting. As is shown by this case, depression fill is unstable when its downslope part is cut artificially or naturally.

Figure 4C shows the laser scanner map of the southwestern bank of the River Hokkawa (Fig. 1). Two landslides of depression fill occurred on slopes above knick points of hollows located at the heads of ravines, retrogressing the knick points upslope (cross section of Fig. 4C). This type of landslide has somehow a similar morphology of bowl-like depression. We performed portable-cone penetration tests upslope of the heads of these landslide scars; the results are shown by the blow number (N_{10}), which is the force necessary to penetrate a metal cone 2.5 cm in diameter for 10 cm by hitting it with a 50-cm free-falling weight of 5 kg. This test clearly showed the presence of a very loose layer with only a few N_{10} values about 1-m deep in the slopes, even more than 20 m from the knick points, indicating that underground erosion proceeded upslope from the knick point (Fig. 6). These underground erosions occurred with catchment areas of as small as 1,200 and 2,000 m^2. This result strongly suggests that the next slide will occur upslope of these knick points. The gradients of the slopes with underground erosion were 12° and 15°.

Areal susceptibility evaluation from the airborne laser scanner

As described before, an airborne laser scanner working under good conditions, for example, in the absence of tree leaves, can identify old landslides as well as new ones, providing landslide density and area, which could be used as indices of long-term landslide susceptibility in a wide area. For example, the area of this study had a landslide density of at least 117 within 1 km^2 of slopes steeper than 20° before the 1998 event, and a new landslide density of 233 km^2 after the event. In addition, the landslide area share over the area of slopes steeper than 20° was 5.09% for the landslides generated during the 1998 event, and 2.96% for old landslides. These numbers are quite large and of about the same order as the landslide density and landslide area share of the devastating disaster that occurred in a weathered granite area of Nishi Mikawa (or Obara Village), central Japan in 1972; which had a density of 294 km^2 and a area share of 4.30% for new landslides

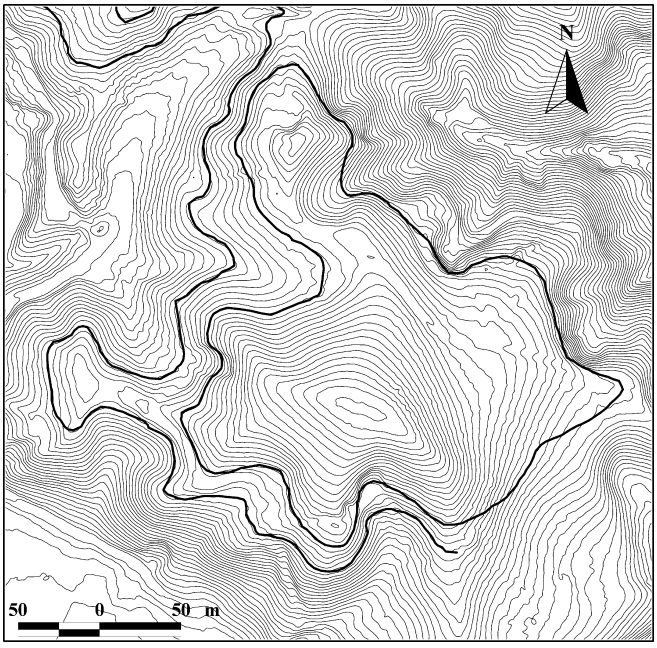

Fig. 5 Terrace-like landform along the trace of pumice and scoria beds on the mudflow deposits and tuff. The top and the base of the mudflow deposit are shown by *solid lines*. Contour interval is 1 m

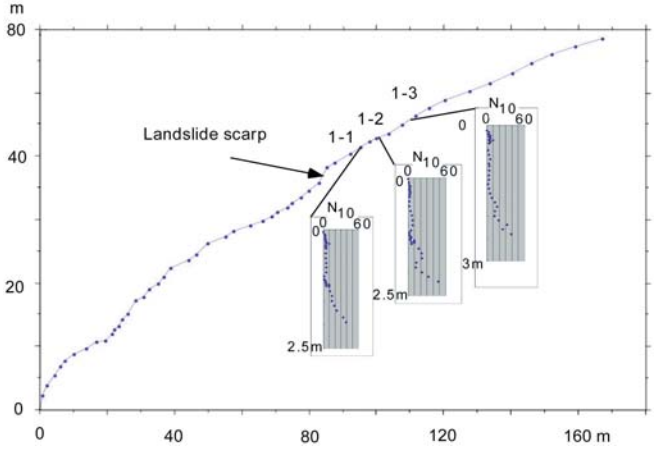

Fig. 6 Portable cone penetration test results at site 2 on the south bank of the Hokkawa River

at the time of the event, and at least 114 km^2 and 1.60% before the event (Tobe and Chigira 2004; Duan, personal communication). The time interval, in which the detected landslide occurred, could not be specified, but it seems to be on the order of tens or hundreds of years on the basis of the weathering rate—production rate of slide materials (Shimokawa 1984). Anyway, a constantly high landslide density suggests high susceptibility.

Conclusions

Airborne laser scanning was successfully performed to detect new and old landslide scars and small-scale geomorphic features in the 1998 Fukushima rainstorm disaster area. Three types of landslide occurred, of which morphology is related to landslide mechanism.

The first type of landslide was in alignment with the trace of permeable pumice and scoria beds that overlie impermeable vapor-phase crystallized ignimbrite and mudflow deposits. This hydrogeological structure allowed rainwater to infiltrate through the permeable materials, then move laterally, and then gush out along the surface trace of the permeable materials, generating landslides. This alignment becomes much clearer if we add old landslides detected by the laser scanner to the new 1998 landslides. The landslides of this type have very characteristic morphology. The source area is an amphitheater or bowl-like depression with a very gentle lower part and a relatively steep upper part; almost no debris remained within the scar. This morphology was clearly identified by the airborne laser scanner and seems to be characteristic of landslides occurring at sites with a hydrogeological structure in which permeable materials horizontally overlie impermeable materials. The successive occurrence and retrogression of the landslide scars of this type made 10–20-m-wide terrace-like features.

The second type of landslide was of heavily weathered tuff and debris, with a planar landslide scar on exfoliated tuff and a U-shaped scarplet upslope. The basic cause of this type of landslide was the weathering profile of the tuff, which forms the bedrock in this area. The basic conditions for this type of landslide exist widely in this area.

The third type of landslide were landslides of depression fill, which slid at knick points. The knick points and the landslide scars were also identified by airborne laser scanning.

Using a laser scanner technique in coniferous or deciduous trees in a season with fewer leaves allows one to recognize landslide occurrences within tens of years, providing a record of landslide susceptibility. The landslide density and landslide area share on those slopes steeper than 20 in the investigated area were at least 117 km^2 and 2.96% before the event and increased by 233 km^2 and 5.09% by the event.

Acknowledgment

This research was funded by the Ministry of Education, Culture, Sports, Science and Technology (MEXT)—Special Coordination Fund for Promoting Science and Technology, Aerial Prediction of Earthquake and Rain Induced Flow Phenomena (APERIF Project), Principal Investigator: Kyoji SASSA. We appreciate the discussion and the help in the field survey of Noriyuki Chiba of Tohoku Gakuin University and Jun Umemura of Nihon University. We are also grateful to Tatsuro Chiba, of Asia Air Survey, for his help in the imaging analysis of DEM data.

References

Bates PD, Marks KJ, Horritt MS (2003) Optimal use of high-resolution topographic data in flood inundation models. Hydrol Process 17:537–557

Carrara A, Cardinali M, Detti R, Guzzetti F, Pasqui V, Reichenbach P (1991) GIS techniques and statistical models in evaluating landslide hazard. Earth Surf Process Landf 16:427–445

Chigira M (2002) Geologic factors contributing to landslide generation in a pyroclastic area: August 1998 Nishigo Village, Japan. Geomorphology 46:117–128

Chigira M, Nakamoto M, Nakata E (2002) Weathering mechanisms and their effects on the landsliding of ignimbrite subject to vapor-phase crystallization in the Shirakawa pyroclastic flow, northern Japan. Eng Geol 66:111–126

Dai FC, Lee CF (2003) A spatiotemporal probabilistic modeling of storm-induced shallow landsliding using aerial photographs and logistic regression. Earth Surf Process Landf 28:527–545

French JR (2003) Airborne lidar in support of geomorphological and hydraulic modeling. Earth Surf Process Landf 28:321–335
Gupta RP, Joshi BC (1989) Landslide hazard zoning using the GIS approach: a case study from the Ramganga catchment, Himalayas. Eng Geol 28:119–131
Kennet M, Eiken T (1997) Airborne measurement of glacier surface elevation by scanning laser altimeter. Ann Glaciol 24:293–296
Lane SN, Westawau RC, Hicks DM (2003) Estimation of erosion and deposition volumes in a large, gravel-bed, braided river using synoptic remote sensing. Earth Surf Process Landf 28:249–271
McKean J, Roering J (2004) Objective landslide detection and surface morphology mapping using high-resolution airborne laser altimetry. Geomorphology 57:331–351
Montgomery DR, Dietrich WE (1994) A physically based model for the topographic control of shallow landsliding. Water Resour Res 30:1153–1171
Montgomery DR, Schmidt KM, Greenberg HM, Dietrich WE (2000) Forest clearing and regional landsliding. Geology 28:311–314
Okimura T, Kawatani T (1987) Mapping of the potential surface-failure sites on granite slopes. In: Gardner E (ed) International geomorphology. Wiley, Chichester, pp 121–138
Ridgway JR, Minster JB, Williams N, Bufton JL, Krabill WB (1997) Airborne laser altimeter survey of Long Valley, California. Geophys J Int 131:267–280
Shimokawa E (1984) Natural recovery process of vegetation on landslide scars and landslide periodicity in forested drainage basins. Proceedings of the Symposium on Effects of Forest Land Use on Erosion and Slope Stability. Honolulu, Hawaii, pp 99–107
Suzuki T (1992) Tephrochronological study on Nasu Volcano. Bull Volcanol Soc Japan 37:251–263
Suzuki T, Fujiwara O, Danhara T (1998) Fission track ages of eleven Quaternary Tephras in north Kanto and south Tohoku regions, central Japan. Quat Res 37:95–106
Tobe H Chigira M (2004) Relationships between landslide densities detected by airborne laser scanner and the petrological texture of granitic rocks. To be presented at the 32nd International Geological Congress, August 2004, Florence, Italy
Umemura J, Mori Y, Maruyama K, Yoshioka D (1999) Sediment disasters due to the southern Fukushima heavy rain fall 1998, August. Tohoku J Nat Disast Sci 35:1–6
Wu W, Sidle RC (1995) A distributed slope stability model for steep forested basins. Water Resour Res 31:2097–2110
Yoshida H, Takahashi M (1991) Geology of the eastern part of the Shirakawa pyroclastic flow field. J Geol Soc Japan 97:231–249

M. Chigira (✉) · F. Duan
Disaster Prevention Research Institute,
Kyoto University,
611-0011 Gokasho, Uji, Japan
e-mail: chigira@slope.dpri.kyoto-u.ac.jp
Tel.: +81-774-384100
Fax: +81-774-384105

H. Yagi
Yamagata University,
1-4-12 Koshirakawa, 990-8560, Yamagata, Japan

T. Furuya
Chiba University,
1-33 Yayoi, 263-8522 Inage, Chiba, Japan